Available online at www.sciencedirect.com
ScienceDirect
Scripta Materialia 60 (2009) 52–55
Scripta MATERIALIA
www.elsevier.com/locate/scriptamat

Influence of stacking fault energy on deformation mechanism and dislocation storage capacity in ultrafine-grained materials

Z.W. Wang,[a] Y.B. Wang,[a] X.Z. Liao,[a,*] Y.H. Zhao,[b] E.J. Lavernia,[b] Y.T. Zhu,[c,*] Z. Horita[d] and T.G. Langdon[e,f]

[a]*School of Aerospace, Mechanical and Mechatronic Engineering, The University of Sydney, Sydney, NSW 2006, Australia*
[b]*Department of Chemical Engineering & Materials Science, University of California, Davis, CA 95616, USA*
[c]*Department of Materials Science and Engineering, North Carolina State University, NC 27695, USA*
[d]*Department of Materials Science and Engineering, Faculty of Engineering, Kyushu University, Fukuoka 819-0395, Japan*
[e]*Departments of Aerospace and Mechanical Engineering and Materials Science, University of Southern California, Los Angeles, CA 90089-1453, USA*
[f]*Materials Research Group, School of Engineering Sciences, University of Southampton, Southampton SO17 1BJ, UK*

Received 1 July 2008; revised 12 August 2008; accepted 28 August 2008
Available online 9 September 2008

Partial dislocation emission from grain boundaries in metals with medium-to-high stacking fault energies is observed primarily in the grain size range of a few tens of nanometers. Here we report that a reduction in the stacking fault energy permits the emission of partial dislocations from grain boundaries in ultrafine-grained materials with grain sizes significantly larger than 100 nm and this produces twinning. Such twins are effective in increasing the dislocation storage capacity, which may be used to improve the ductility.

Keywords: Ultrafine-grained materials; Deformation mechanism; Stacking fault energy

The mechanical properties of nanostructured (ns) materials are determined by the active deformation mechanisms, which depend upon their microstructures. Extensive theoretical and experimental investigations have been conducted to understand the deformation mechanisms in ns materials and two general conclusions are now established:

(1) at the smallest grain sizes (e.g. <10 nm), deformation occurs mainly through grain boundary rotation and sliding [1–5], which is believed responsible for the observed reverse Hall–Petch effect, i.e. lower strength with smaller grain sizes [6–8]; and
(2) the emission of partial dislocations from grain boundaries plays a major role in the deformation of face-centered cubic (fcc) metals with grain sizes of a few tens of nanometers [5,7,9–12]. This consequently produces deformation twins in nanocrystalline fcc metals, such as Cu [5,12], Al [10,11] and Ni [13], which have medium-to-high stacking fault (SF) energies. These fcc metals usually do not twin when deformed at room temperature at low strain rates in their coarse-grained states because conventional dislocation sources, such as Frank–Read sources, operate in the interiors of the large grains.

Critical grain sizes for deformation twinning have been observed in nanocrystalline fcc metals above which no deformation twins are formed by partial dislocation emission from the grain boundaries [5,14]. For example, in pure Cu deformed by high-pressure torsion (HPT), deformation twins were observed only in grains smaller than 50 nm [5]. One exception was recently reported in a single crystal of Cu deformed by equal channel angular pressing (ECAP) for one pass, where twins were observed in elongated grains wider than 200 nm [15]. This was attributed to the specific crystal orientation of the single crystal that produced a maximum resolved shear stress for a twinning system during ECAP. Although Huang et al. [16] reported deformation twins in submicron grains of ECAP Cu, the possibility that the twins were actually generated before the grains

* Corresponding authors. Tel.: +61 2 9351 2348; fax: +61 2 9351 7060 (X.Z.L.); tel.: +1 919 513 0559; fax: +919 515 3419 (Y.T.Z); e-mail addresses: xliao@usyd.edu.au; ytzhu@ncsu.edu

1359-6462/$ - see front matter © 2008 Acta Materialia Inc. Published by Elsevier Ltd. All rights reserved.
doi:10.1016/j.scriptamat.2008.08.032

reached the submicron size cannot be ruled out. Most other published reports on ECAP ultrafine-grained Cu with grain sizes larger than 100 nm show no deformation twin [17], thereby reinforcing the impression that deformation twinning usually fails to occur in grains larger than ~100 nm. These observations raise a question: can partial dislocation emission from grain boundaries occur in ultrafine-grained (UFG) materials having grain sizes larger than 100 nm? If the answer is in the affirmative, deformation twinning from grain boundaries will probably occur. This leads to another question concerning the effectiveness of deformation twinning in enhancing the dislocation storage capability. This latter question is important for the ductility of UFG materials because dislocation accumulation will improve the strain hardening and consequently improve the ductility [18,19].

In this letter, we report a transmission electron microscopy (TEM) investigation showing that, by reducing the SF energy, partial dislocation emissions from grain boundaries are possible even in grains as large as ~200 nm. In this size range, the full dislocation motion is effectively blocked by the SFs and nano-twins generated by partial dislocation emission from the grain boundaries. As a result, the dislocation storage capacity is maintained in UFG materials with low SF energies. It is anticipated that this will improve the mechanical properties of these materials, especially the ductility.

A Cu–10 wt.% Zn alloy with a SF energy of 35 mJ m^{-2}, which is much lower than that of Cu (78 mJ m^{-2}) [20], was used in this investigation. An alloy disk with a thickness of 0.8 mm and a diameter of 10 mm was processed by high-pressure torsion (HPT) for five revolutions at room temperature under an applied pressure of 6 GPa. TEM specimens were sectioned from the disk edge and prepared by mechanical grinding to a thickness of about 30 μm followed by ion-polishing at liquid nitrogen temperature using a Fischione 3000 ion polisher with an Ar accelerating voltage of 4.0 kV. TEM investigations were carried out using a JEOL 3000 F transmission electron microscope operating at 300 kV. Earlier reports described the grain configurations [21] and the microstructural characteristics [22] of this alloy after processing by HPT.

Figure 1a shows a typical TEM bright-field image of the HPT sample. The grain sizes in the sample are mainly in the range of ~50–200 nm although grain sizes of ~10–20 nm are also found in small quantities. Careful examination of a large number of grains by tilting to a <0 1 1> orientation suggests that nano-twins and/or SFs are present in most of the grains and only a small fraction of the grains are free of twins and SF. One twinned grain, having a grain size of ~180 nm, is marked with a letter "A" in Figure 1a. The images of a grain without any twins/SFs and a grain with high density of twins/SFs are shown in Figure 1b and c, respectively.

Dislocation densities in grains with and without twins/SFs were examined from high-resolution TEM images using the method described earlier [23]. The dislocation density in grains with twins/SFs was ~2–5 × 10^{16} m^{-2}, which is many times higher than in grains without any twins/SFs (~0.5 × 10^{16} m^{-2}). This

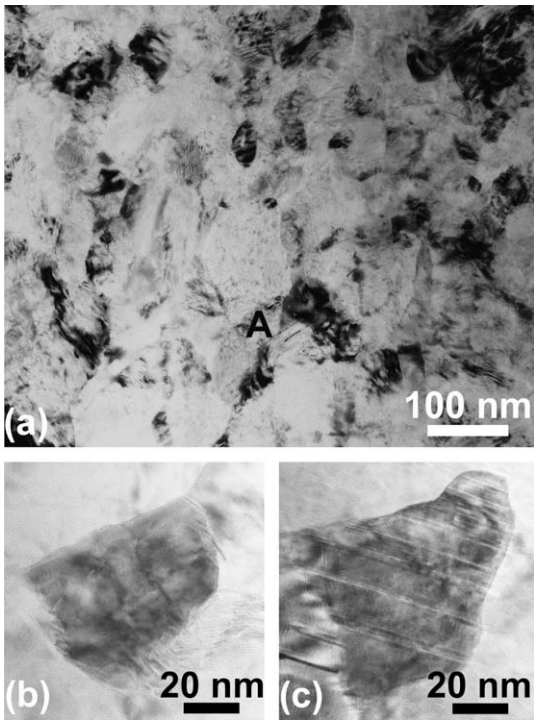

Figure 1. (a) A typical TEM bright-field image of the HPT sample showing the grain size range of 50–200 nm. A black letter "A" marks a grain of around 180 nm with nano-twins. (b) A typical image of a grain without any twin/stacking fault. (c) A typical image of a grain with high density of nano-twins/stacking faults.

strongly suggests that the twins and SFs act as effective sites for blocking slipping and storing dislocations.

While the twin boundaries visible in coarse-grained materials are normally atomically flat, atomic steps are frequently observed on the twin boundaries of nanocrystalline materials [12]. This difference in the twin boundary morphologies is caused by the different twin formation mechanisms that operate in coarse-grained and nanocrystalline materials, respectively. Accordingly, the twin boundary morphology may be used to investigate twin formation. The detailed morphological investigation conducted here suggests that the nano-twins found in grains in the size range of ~50–200 nm are formed through partial dislocation emissions from grain boundaries. Figure 2a shows a typical low magnification image of a nano-twin found in a grain of ~120 nm. As shown in Figure 2a, the width of the nano-twin decreases from the top (marked with B) to the bottom (marked with C). These top and bottom images are enlarged in Figure 2b and c, respectively. While the top end of the nano-twin in Figure 2b includes 10 {1 1 1} layers with a width of 2.1 nm wide, the bottom end of the nano-twin in Figure 2b comprises only two {1 1 1} layers.

The observed variation in twin thickness in Figure 2 can be explained by the successive emission of partial dislocations from the top grain boundary [24,25]. Those emitted later are stopped within the grain either because the external force driving the motion of the partial dislocations was not sufficiently high to drive them across the grain or because the external force was withdrawn before the partial dislocations reached the other end of

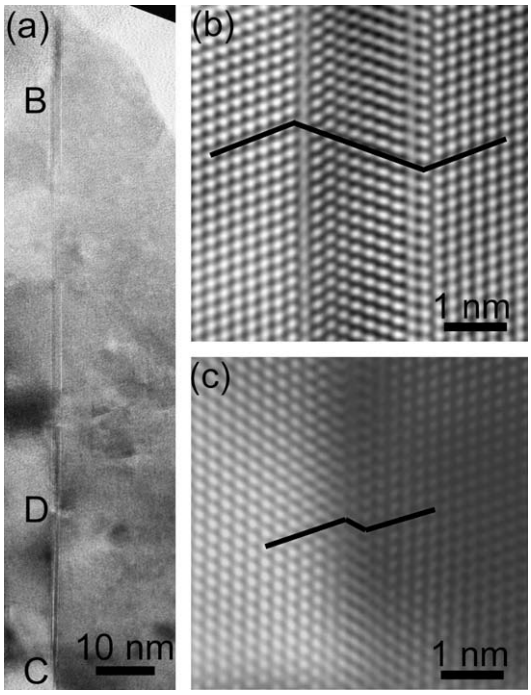

Figure 2. (a) A typical low magnification image of a nano-twin found in a grain of ~120 nm. (b) A magnified image of the top end of (a), which is marked with a "B", showing the twin thickness of 10 atomic layers. (c) A magnified image of the bottom end of (a), which is marked with a "C", showing a twin of only two atomic layers. The letter "D" marks the area that is further magnified in Figure 3.

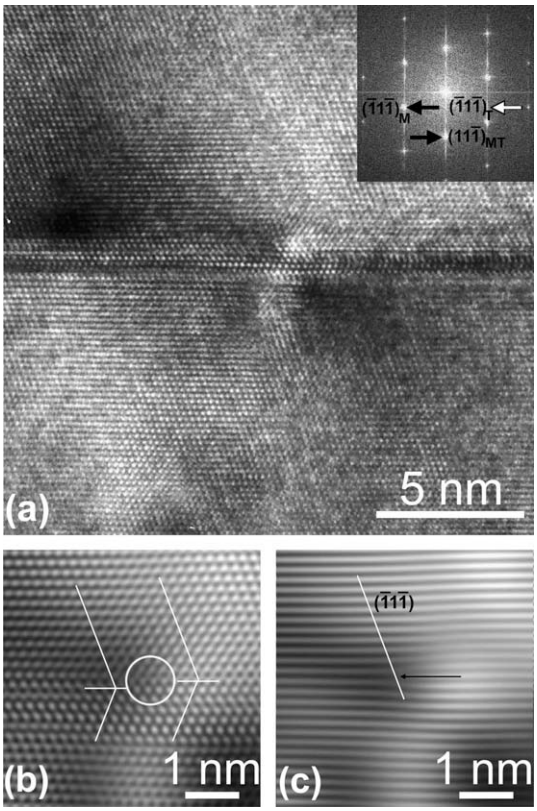

Figure 3. (a) A high-resolution TEM image of the nano-twin area marked with a "D" in Figure 2a. A twin thickness variation occurs at the center of the image. Inserted at the upper right corner is the Fourier transformation of the image. (b) A Fourier-filtered image of the central part of (a) showing clearer lattice fringes. A white circle marks an area with imperfection. White lines that are parallel to {1 1 1} planes indicate a twin boundary shift. (c) A one-dimensional Fourier-filtered image of the same area. A projected full dislocation component is indicated by a black arrow, and a white line indicates the {1 1 1} plane on which the full dislocation glided before meeting a partial dislocation.

the grain. Furthermore, dislocation interactions can also stop partial dislocations and prevent them from slipping to the other end of the grain. Figure 3a shows a magnified image of the area marked "D" in Figure 2a. It presents an example of partial–full dislocation interaction that blocks the motion of a partial dislocation. A thin twin lamella is seen in Figure 3a and the lamella thickness varies at the center of the image. Inserted at the upper right corner of Figure 3a is the Fourier transformation of the image with the very weak $(\bar{1}\,1\,\bar{1})_T$ spot (indicated with a white arrow) generated from the twin, the $(\bar{1}\,1\,\bar{1})_M$ spot (marked with a black arrow) from the matrix, and the $(1\,1\,\bar{1})_{MT}$ spot (also marked with a black arrow) contributed by both the matrix and the twin. To see the detailed structure of the area with the twin thickness variation, a Fourier-filtered image of the area is shown in Figure 3b, in which a white circle marks an area where lattice disorder occurs. It is clear that the upper twin–matrix boundary at the right of the white circle is one atomic layer higher than that at the left of the white circle, thereby indicating that the partial dislocation that generated the outermost twin layer stopped within the area of the white circle. However, the lattice disorder within the white circle is too complex and extensive to be caused by a $\frac{1}{6}<1\,1\,2>$ type partial dislocation. In fact, the one-dimensional Fourier-filtered image obtained from the $\pm(1\,1\,\bar{1})_{MT}$ spots in Figure 3c, which is in the same area as Figure 3b, clearly indicates the projected component of a full dislocation (indicated by the black arrow) at the center of the image. Combining information obtained from Figure 3b and c, we conclude that the partial dislocation that glided from the right to the left and generated the outermost twin layer was stopped by a full dislocation that glided on $(\bar{1}\,1\,\bar{1})$ (as indicated by the straight white line in Figure 3c). When the partial dislocation interacted with the full dislocation, a new Burgers vector was created which was not lying in any glide plane and therefore represented a sessile dislocation.

Because of the computational limitations, most molecular dynamics (MD) simulations showing partial dislocation emissions from grain boundaries were carried out for structures with grain sizes smaller than 100 nm [7–9]. Furthermore, no MD simulation has been carried out for materials with low SF energies. Previous experimental results on Cu [5,12] (which was processed under similar conditions to that of the Cu–10 wt.% Zn alloy reported here), Al [10,11] and Ni [13] also show that partial dislocation emissions occur only in grains smaller than 100 nm. The discovery reported in this letter indicates that the grain size for activating partial dislocation emissions from grain boundaries is a function of the SF energy and can be much larger than 100 nm for materials with low SF energies. This discovery is very important because it is believed that the conven-

tional deformation mechanisms for coarse-grained materials remain active in grains larger than ~100 nm, as evidenced by the high dislocation densities in twinned and untwined grains in the present study. This observation implies that, for materials with low SF energies, there exists a size range in which the two deformation mechanisms of partial dislocation emission from grain boundaries and full dislocation slip and multiplication are able to function simultaneously.

Ma et al. [26] and Lu et al. [27] reported that pre-existing nanoscale twin boundaries can effectively increase the strain rate sensitivity due to an interaction between the twin boundaries and full dislocations that prevents the full dislocations from moving to and disappearing at the grain boundaries. Therefore, this significantly increases the dislocation storage capacity of the materials. Unfortunately, the introduction of pre-existing growth twins in large bulk nano/UFG materials for structural applications remains a challenge. The discovery reported in this letter provides an effective way, by reducing the SF energy of materials via alloying, to take advantage of twin boundary-full dislocation interactions in more materials and thereby increase the strain hardening and strain rate sensitivity of these materials.

The authors acknowledge the facilities and technical assistance from the staff in the Australian Microscopy & Microanalysis Facility at the Electron Microscope Unit, The University of Sydney. This project is financially supported by the Australian Research Council (DP0772880; Z.W.W., Y.B.W. and X.Z.L.); the Office of Naval Research (N00014-04-1-0370 and N00014-08-1-0405; Y.H.Z. and E.J.L.), with Dr. Lawrence Kabacoff as the program officer; the DOE IPP program (Y.T.Z.); a Grant-in-Aid for Scientific Research from MEXT, Japan, in the Priority Area "Giant Straining Process" (Z.H.); and by the U.S. Army Research Office under Grant No. W911NF-05-1-0046 (T.G.L.).

[1] J. Schiøtz, F.D. Ditolla, K.W. Jacobsen, Nature 391 (1998) 561.
[2] V. Yamakov, D. Wolf, S.R. Phillpot, H. Gleiter, Acta Mater. 50 (2002) 61.
[3] Z.W. Shan, E.A. Stach, J.M.K. Wiezorek, J.A. Knapp, D.M. Follstaedt, S.X. Mao, Science 305 (2004) 654.
[4] Y.B. Wang, B.Q. Li, S.X. Mao, M.L. Sui, Appl. Phys. Lett. 92 (2008) 011903.
[5] X.Z. Liao, Y.H. Zhao, Y.T. Zhu, R.Z. Valiev, D.V. Gunderov, J. Appl. Phys. 96 (2004) 636.
[6] K. Lu, Mater. Sci. Eng. R16 (1996) 161.
[7] V. Yamakov, D. Wolf, S.R. Phillpot, A.K. Mukherjee, H. Gleiter, Nature Mater. 3 (2004) 43.
[8] J. Schiotz, K.W. Jacobsen, Science 301 (2003) 1357.
[9] H. Van Swygenhoven, M. Spacer, A. Caro, Acta Mater. 47 (1999) 3117.
[10] X.Z. Liao, F. Zhou, E.J. Lavernia, S.G. Srinivasan, M.I. Baskes, D.W. He, Y.T. Zhu, Appl. Phys. Lett. 83 (2003) 632.
[11] X.Z. Liao, F. Zhou, E.J. Lavernia, D.W. He, Y.T. Zhu, Appl. Phys. Lett. 83 (2003) 5062.
[12] X.Z. Liao, Y.H. Zhao, S.G. Srinivasan, Y.T. Zhu, R.Z. Valiev, D.V. Gunderov, Appl. Phys. Lett. 84 (2004) 592.
[13] X.L. Wu, Y.T. Zhu, Appl. Phys. Lett. 89 (2006) 03192.
[14] X. Wu, Y.T. Zhu, E. Ma, Appl. Phys. Lett. 88 (2006) 121905.
[15] W.Z. Han, S.D. Wu, S.X. Li, Z.F. Zhang, Appl. Phys. Lett. 92 (2008) 221909.
[16] C.X. Huang, K. Wang, S.D. Wu, Z.F. Zhang, G.Y. Li, S.X. Li, Acta Mater. 54 (2006) 655.
[17] S. Komura, Z. Horita, M. Nemoto, T.G. Langdon, J. Mater. Res. 14 (1999) 4044.
[18] Y.H. Zhao, X.Z. Liao, S. Cheng, E. Ma, Y.T. Zhu, Adv. Mater. 18 (2006) 2280.
[19] Y.H. Zhao, Y.T. Zhu, X.Z. Liao, Z. Horita, T.G. Langdon, Appl. Phys. Lett. 89 (2006) 121906.
[20] Y.H. Zhao, X.Z. Liao, Y.T. Zhu, Z. Horita, T.G. Langdon, Mater. Sci. Eng. A 410–411 (2005) 188.
[21] T. Ungár, L. Balogh, Y.T. Zhu, Z. Horita, C. Xu, T.G. Langdon, Mater. Sci. Eng. A444 (2007) 153.
[22] L. Balogh, T. Ungár, Y. Zhao, Y.T. Zhu, Z. Horita, C. Xu, T.G. Langdon, Acta Mater. 56 (2008) 809.
[23] X.Z. Liao, J.Y. Huang, Y.T. Zhu, F. Zhou, E.J. Lavernia, Philos. Mag. 83 (2003) 3065.
[24] Y.T. Zhu, X.Z. Liao, S.G. Srinivasan, Y.H. Zhao, M.I. Baskes, F. Zhou, E.J. Lavernia, Appl. Phys. Lett. 85 (2004) 5049.
[25] Y.B. Wang, M.L. Sui, E. Ma, Philos. Mag. Lett. 87 (2007) 935.
[26] E. Ma, Y.M. Wang, Q.H. Lu, M.L. Sui, L. Lu, K. Lu, Appl. Phys. Lett. 85 (2004) 4932.
[27] L. Lu, R. Schwaiger, Z.W. Shan, M. Dao, K. Lu, S. Suresh, Acta Mater. 53 (2005) 2169.